

## Exploring Conditions Leading to Wintertime Ozone Episodes in Natural Gas Fields in Mountain Valleys

Yuling Wu\* and Arastoo Pour-Biazar

Earth System Science Center, University of Alabama in Huntsville, Huntsville, AL, USA

Bernhard Rappenglück

Department of Earth and Atmospheric Sciences, University of Houston, Houston, TX, USA

Robert A. Field

Department of Atmospheric Science, University of Wyoming, Laramie, WY, USA

### 1. INTRODUCTION

High ozone production in wintertime has been reported in natural gas producing regions in the river valleys in Wyoming and Utah high lands (e.g. Schnell et al., 2009; Carter and Seinfeld, 2012; Rappenglück et al., 2014; Ahmadov et al., 2015; Field et al., 2015). Prior research of observational data analysis and modeling studies has identified common factors such as shallow boundary layer and low wind that results in augmented concentration of ozone precursors, and enhanced photolysis rates due to combination of high snow albedo, high solar zenith angles and high altitudes, leading to high wintertime ozone productivity in these natural gas producing fields. Results from the research also show high variability in chemical compositions that are critical to ozone production, for example, VOC-limited vs NO<sub>x</sub>-limited chemical regimes; large contribution to ozone productivity from the aromatic species vs strong contribution from other VOCs on top of the aromatics.

In this study, we discuss the different conditions at the two monitoring sites (8 km apart from each other) in the vicinity of the natural gas producing field in the Upper Green River Basin (UGRB) in Wyoming that lead to high ozone in the wintertime. Model simulation with sensitivity study is employed to study the conditions at one of the two sites that recorded much lower concentrations of the ozone precursors but had high ozone production. The site has not been the focus in prior research.

### 2. OBSERVATION

The UGRB in Wyoming is located at ~2000m elevation and surrounded by mountain ranges to its west and northwest. Oftentimes, there is snow

cover in the wintertime (Rappenglück et al., 2014). Oil and gas extraction operations are running continuously, putting out considerable amounts of NO<sub>x</sub> and various VOC species, depending on the facilities. Peak ozone concentration over 150 ppb was reported at multiple WDEQ monitoring sites, including the tethered balloon site (in source

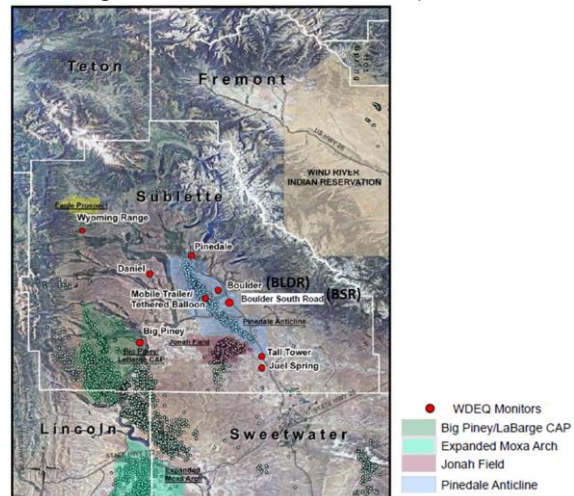


Fig. 1. Map of location of sources of the gas fields, and the monitoring sites in the Upper Green River Basin, Wyoming. VOC species and NO<sub>x</sub> emissions are facilities dependent and thus are not necessarily co-emitted. (Figure reproduced from Rappenglück et al., 2014).

region) and the BLDR site (near sources) during the late winter of 2011. While lower NO<sub>x</sub> and much less VOC (an order of magnitude smaller) were reported at the BSR site, which is another monitoring site only 8km from the BLDR site, excessive ozone production with maximum of ~120 ppb was observed at this site (Fig. 2) during the same period of 2011. Intriguingly, the observation shows a weak correlation of NO<sub>x</sub> and VOC, but strong correlation (concurrency) of ozone, between the BLDR and the BSR sites (Fig. 3).

\*Corresponding author: Yuling Wu, ESSC/NSSTC, 320 Sparkman Drive, Room 3078; Huntsville, AL 35895; e-mail: [wuy@nsstc.uah.edu](mailto:wuy@nsstc.uah.edu)

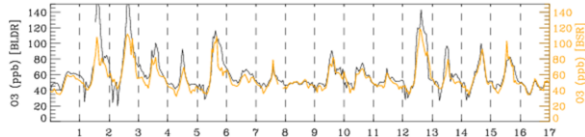


Fig. 2. Observed hourly ozone concentration at the BLDR and the BSR sites.

The wide range of the NMHC/NO<sub>x</sub> ratio in Fig. 4 and the scattering in NO<sub>x</sub> and NMHC in Fig. 3 shows the high variability of the chemical composition at these vicinity sites of the source region. As oil and gas extraction includes operations of different facilities that consist of drill rigs, production equipment and compressor stations, heaters, trucks, etc. Emissions from different facilities possess dissimilar VOCs and NO<sub>x</sub> mixtures. The high variability thus suggests shifting winds that advect the pollutants from different facilities at various locations.

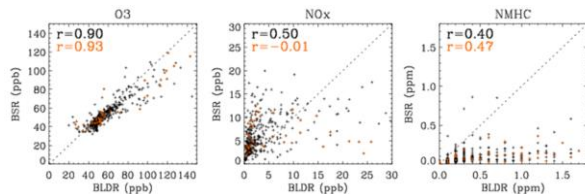


Fig. 3. Correlation of chemical species between the BLDR and the BSR sites. Black for the time period in Fig. 1 and orange for the period in Fig. 5.

It is shown that not only were VOC (NMHC) and NO<sub>x</sub> much different at BSR than at BLDR, the ratio of VOC/NO<sub>x</sub> (Fig. 4), which is closely related to ozone production, was also quite distinct at the two sites, with average VOC/NO<sub>x</sub> < 20 most of the time of the day at BSR, indicating VOC-limited chemistry. The average VOC/NO<sub>x</sub> ratio at BSR was nearly an order of magnitude smaller than at BLDR. On average, the latter was between 100 and 300 for most of the time of the day, indicating a more NO<sub>x</sub>-limited chemistry regime. In general, however, observed ozone concentration was only a little lower at the BSR site than the BLDR site (Fig. 2 and 3).

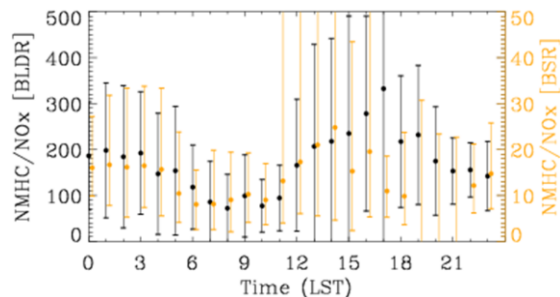


Fig. 4. Average ratio of NO<sub>x</sub>/NMHC at the BLDR and the BSR sites for the period shown in Fig. 2. Vertical bars mark the range of standard deviation.

Figure 5 shows an example of how distinct the conditions are at the two sites on Mar 12, 2011. At BSR, moderate VOCs (~0.1-0.2 ppm) and NO<sub>x</sub> (~10 ppb) were observed during the daytime hours with some VOC spikes in the afternoon. At BLDR, VOCs had a couple of spikes before daylight and several peaks around noon and afternoon while NO<sub>x</sub> peaked after midnight (~25 ppb) and had another peak of ~10 ppb before noon. The afternoon low NO<sub>x</sub> at BLDR might be due to NO<sub>x</sub> reacting away with the abundant radicals produced by high VOCs and/or that the site was in the airflow coming from sources of low NO<sub>x</sub>. Ozone peaked shortly past noon at both locations, then dropped swiftly (reduction of 35 ppb in the afternoon) and steadily after the peak at BSR and rapidly in early afternoon and more sharply in the evening at BLDR. The March 12, 2011 ozone episode at BSR is selected for model simulation study.

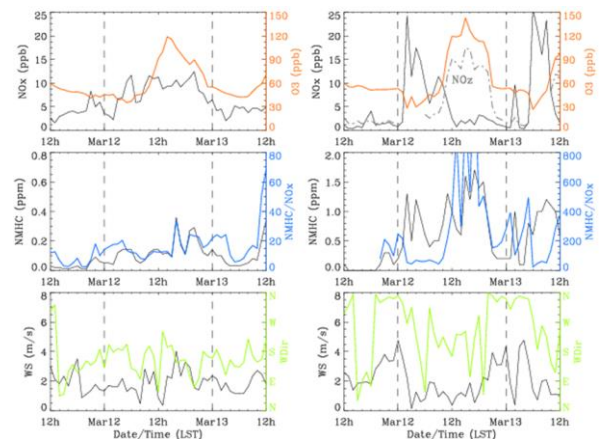


Fig. 5. Chemical and Met. conditions at BSR (left panels) and BLDR (right panels) for the Mar 12, 2011 ozone episode.

### 3. DESCRIPTION OF MODEL SIMULATION

The present study uses the Single Column Model (SCM) of the Weather Research and Forecast model with chemistry (WRF-chem) v3.7 to simulate the ozone episode of March 12, 2011, observed at the BSR site. The simulation is initialized by vertical profiles obtained from the reanalysis data of the North American Mesoscale Forecast System (NAM) for the location and verified with the tethered balloon observation. The NAM data has a horizontal grid spacing of 12 km. In order to resolve the shallow wintertime boundary layer, the simulation is set up with 100 vertical layers, with a 13m first layer and (10, 20, 30) layers below (160, 365, 640) m, initially. The YSU scheme for PBL physics, in junction with the Monin-Obukhov similarity for surface layer and the

unified 4-layer NOAH scheme for land-surface module are opted for the simulation. The RRTMG radiation scheme is used to calculate the radiative transfer for both the short and long wave radiation. The simulation uses the CBMZ chemical mechanism, which is an extended CB-IV mechanism that includes reactive long-lived VOC species and has 55 species and 134 reactions for the gaseous phase chemistry. Prior to the simulation for the study, a two-day spin-up run is conducted to produce equilibrium background concentrations for ICs.

Photolysis rates (frequencies) are calculated using the Tropospheric Ultraviolet and Visible (TUV) photolysis scheme (Madronich, 1987) within WRF-Chem. As practiced in Ahmadov et al. (2015), we also modified the code to allow for the enhancement of photolysis frequencies due to snow albedo ( $\alpha_{SN}$ ). In simulating the winter ozone episodes in the natural gas producing field in Utah, Ahmadov et al. found that the photolysis rates produced from the TUV scheme in WRF-chem are not high enough to yield ozone production from observation with default values of the surface albedo for bare ground that lies within the range of 0.05–0.15. NO<sub>x</sub> and VOCs are injected on an hourly basis during the simulation to mimic the input of emissions from the gas extraction operations.

A standard run is first established with observation matched NO<sub>x</sub> and VOC that yield observed ozone production with an enhanced ground albedo with snow cover. The albedo was found to be ~0.6, in line with the range used for the earlier period of the late winter in Rappenglück et al. (2014). Sensitivity study is employed to examine the role of ground snow cover albedo ( $\alpha_{SN}$ ), NO<sub>x</sub> emissions, emissions of VOC as a whole, and emissions of different VOC groups, in ozone related chemistry. Ground albedo due to snow cover is tested between 0.1 to 0.8, with the addition of the model default. NO<sub>x</sub> emissions are tested between 0.5x and 1.5x of the standard run values. Emissions of VOC as a whole are also tested between 0.5x and 1.5x of the standard run values. Emissions of the alkane, alkene, and aromatic VOCs are tested at 0.5x, 1.0x and 1.5x of the standard run values.

## 4. SIMULATION RESULTS

### 4.1 The Standard Run

Observed ozone production is reproduced by two similar runs, as shown in Fig. 6. The Epre run

adds only positive emissions during the simulation. However, excessive ozone (and other secondary species) and VOCs remain in the afternoon and overnight and cannot be removed simply by reducing emissions of ozone precursors to zero. Hence, the utilization of both positive and negative emissions in Estd run in an attempt to match observation of the primary species. Nevertheless, the introduction of negative emissions of primary species in the simulation cannot remove secondary species that are already produced. The rapid drop of ozone and non-steady trends of NO<sub>x</sub> and VOC in the afternoon suggest advection of plumes of different chemical composition and age. Each downturn of the trends may signal incoming transport of cleaner airflow. The SCM cannot simulation horizontal advection and transport.

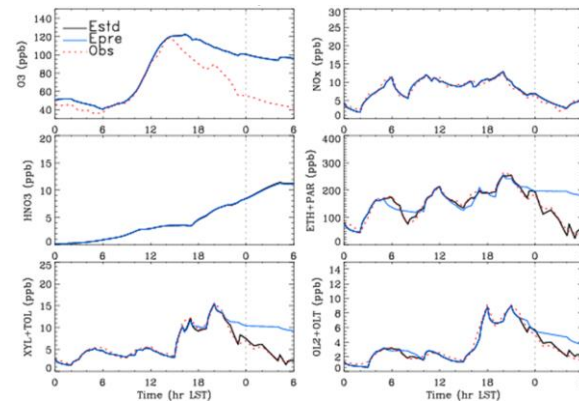


Fig. 6. Simulation results of standard run with  $\alpha_{SN}=0.6$ . Ozone excess ( $\Delta O_3$ ) of 80 ppb (peak of 120 ppb) reached in the early afternoon, recovering from 40 ppb (which is ~10 ppb below background) in the morning.

Among the three major groups of primary VOC species, alkanes were the most massive group in observation for the study episode. However, the reactivity of aromatics with OH dominates during the day (OH is very low at night) as alkenes are relatively low in concentration and alkenes are much less reactive.

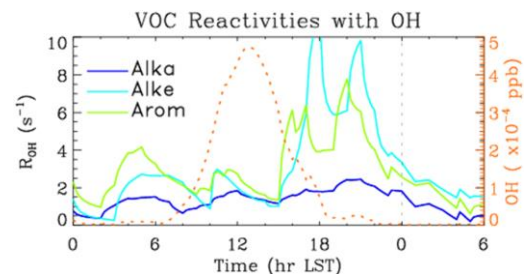


Fig.7. Simulated reactivity of VOC groups with OH and OH concentration in the standard run (std).

### 4.2 Sensitivity Study

Snow covered ground albedo can enhance the atmospheric radiation that in turns, boosts the photolysis rates. The sensitivity runs with  $\alpha_{SN}$  show that the model default bare ground albedo ( $\alpha_{SN} = -$ ) would yield peak  $JNO_2=0.4 \text{ min}^{-1}$  (Fig. 8) which is much smaller than the peak value of  $1.07 \text{ min}^{-1}$  (or  $1.78 \times 10^{-2} \text{ s}^{-1}$ ) calculated for the study period in UGRB in Rappenglück et al. (2014). For the testing range of snow-covered ground albedo of 0.1-0.8, resulting mid-day peak  $JNO_2$  varies from 0.45 to  $1.05 \text{ min}^{-1}$  (Fig. 8), more than doubled.

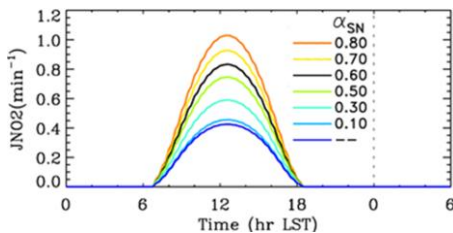


Fig. 8. Simulated photolysis rate of NO<sub>2</sub> in runs testing sensitivity of ozone chemistry to snow albedo.

For tested snow-covered ground albedo (Fig. 9), simulated peak ozone ranges from 85 to 135 ppb ( $\Delta O_3 \sim 45$  to 95 ppb), for  $\alpha_{SN}=0.1$  to 0.8. Ozone production is nearly doubled from the lowest  $\alpha_{SN}$  to the highest  $\alpha_{SN}$ .

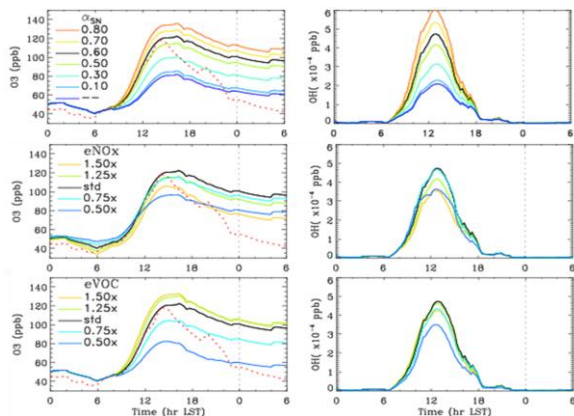


Fig. 9. sensitivity of O<sub>3</sub> and OH to snow albedo (top panels), NO<sub>x</sub> emissions (middle), and VOC emissions (bottom)

For tested NO<sub>x</sub> emissions, simulated peak ozone ranges from 97 to 122 ppb with  $\Delta O_3 \sim 52$  to 82 ppb. The 25 and 50% increase of  $e(NO_x)$  leads to suppression of ozone production as radicals (signified by lowered OH conc. ) produced from VOC are quickly consumed by the paths of the  $NO_x \rightarrow NO_z$  reactions that compete with ozone production (also revealed in Fig. O<sub>3</sub>/NO<sub>z</sub> in Fig. 10). Note that the lowered (raised) NO<sub>x</sub> emissions

also results less (more) depression ozone in the early morning due to titration of O<sub>3</sub>-NO-NO<sub>2</sub>.

For tested VOC emissions, simulated peak ozone ranges from 83 to 133 ppb with  $\Delta O_3$  varying from  $\sim 43$  to 93 ppb. The wider range of ozone production corresponding to  $e(VOC)$  than to  $e(NO_x)$  reflects that the chemistry is in more VOC-limited regimes. Note that NO<sub>x</sub> concentration is VOC-dependent as NO<sub>x</sub> can be removed by termination reaction with radicals produced by VOCs (Fig. 10).

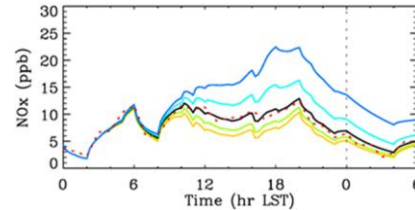


Fig. 10. NO<sub>x</sub> concentration for the VOC emissions sensitivity test. Color coding is the same as in the bottom panels of Fig. 9.

We examine chemical indicators, in addition to ozone and OH. The ratio of HNO<sub>3</sub>/NO<sub>z</sub> decreases with increased VOC emissions (decreased NO<sub>x</sub> emissions). It is particularly the case for the aromatics and alkenes (not shown), indicating the relatively higher production of other NO<sub>z</sub> species (than HNO<sub>3</sub>) with increased VOC in the testing range (Fig. 11).

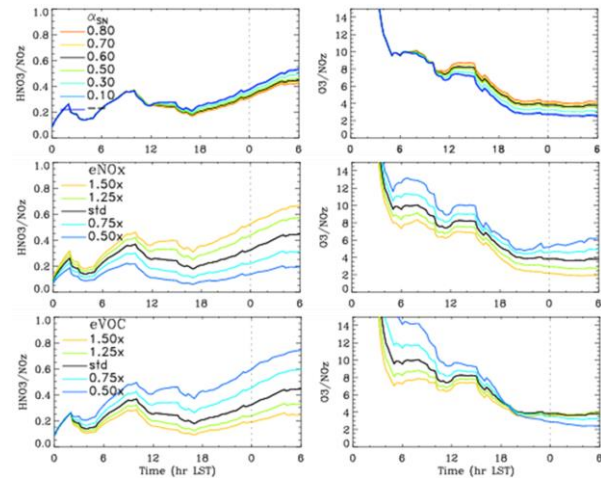


Fig. 11. Same as Fig. 9, but for sensitivity of HNO<sub>3</sub>/NO<sub>z</sub> and O<sub>3</sub>/NO<sub>z</sub>.

O<sub>3</sub>/NO<sub>z</sub> as a photochemical indicator tends to increase with decreased ozone (Sillman and He, 2002). However, it also reflects competition between O<sub>3</sub> and NO<sub>z</sub> production. In the testing range, increased  $\alpha_{SN}$  (enhanced J) boosts all reactions, yielding the difference in O<sub>3</sub>/NO<sub>z</sub> of  $\sim 2$  between the highest and lowest ozone production

runs. Much larger differences in the ratio are seen between the highest and lowest ozone production runs in both e(NO<sub>x</sub>) and e(VOC) sensitivity tests (Fig. 11).

In the 0.5x (1.5x) std emissions test of the three major VOC groups (Fig. 12), the reduction (increase) in ozone production is most significant with reduced (increased) aromatics. i.e. ozone production is most sensitive to aromatics .

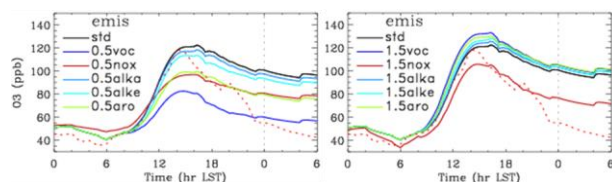


Fig. 12. Sensitivity of ozone production to emissions of various VOC groups, in comparison to emissions of NO<sub>x</sub> and total VOC.

## 5. SUMMARY

Near the sources of non-uniform emissions, the distances from the sources and wind directions can greatly change the chemical composition relevant to ozone chemistry, as showcased in the March 12, 2011 ozone episode at BSR and BLDR sites (Fig. 5).

Model simulation shows the aromatics, among the VOC groups, are the dominant contributor to the photochemistry and ozone production in the Mar12, 2011 ozone episode observed at the BSR site, and alkenes come in a close second while the most massive alkanes make a smaller share of the contribution.

Sensitivity study has shown that ozone production is very sensitive to ground albedo, when accounting for snow cover in the elevated UGRB in Wyoming. Ozone production is boosted from 45 to 95 ppb in the tested range of  $\alpha_{SN}$  of 0.1 to 0.8 based on the March 12, 2011 ozone episode. Ozone production is also very sensitive to VOC emissions, with excess increased from ~ 43 to 93 ppb for 0.5x to 1.5x the emission values in the std run. Ozone production is less sensitive to NO<sub>x</sub> emissions than to VOC emissions for the testing ranges. Increase NO<sub>x</sub> emissions may lead to suppression of ozone production.

Although BSR had much lower VOC and NO<sub>x</sub> concentrations and VOC/NO<sub>x</sub> ratio (an order of magnitude smaller and in the VOC-limited chemical regime), as compared with the same chemical parameters measured at BLDR (and tethered balloon site in the source region), the model simulation shows high ozone production

(maximum of 120 ppb or higher) can be achieved with favorable mix of VOC and NO<sub>x</sub> and metrological condition (near clear sky). Ozone productivity is boosted by enhanced photochemistry due to high surface albedo from ground snow cover. Simulation results show that high snow albedo can more than double ozone production in moderately polluted environment.

## 6. REFERENCES

- Ahmadov, R., McKeen, S., Trainer, M., et al., 2015: Understanding high wintertime ozone pollution events in an oil- and natural gas-producing region of the western US, *Atmos. Chem. Phys.*, 15, 411-429, doi:10.5194/acp-15-411-2015.
- Carter, W. P. L. and Seinfeld, J. H., 2012: Winter ozone formation and VOC incremental reactivities in the Upper Green River Basin of Wyoming, *Atmos. Environ.*, 50, 255–266, doi:10.1016/j.atmosenv.2011.12.025.
- Field, R. A., Soltis, J., McCarthy, M. C., Murphy, S., and Montague, D. C.: Influence of oil and gas field operations on spatial and temporal distributions of atmospheric non-methane hydrocarbons and their effect on ozone formation in winter, *Atmos. Chem. Phys.*, 15, 3527-3542, doi:10.5194/acp-15-3527-2015, 2015.
- Madronich, S., 1987: Photodissociation in the atmosphere, 1. Actinic flux and the effects of ground reflections and clouds, *J. Geophys. Res.-Atmos.*, 92, 9740–9752, doi:10.1029/JD092iD08p09740.
- Rappenglück, B., Ackermann, L., Alvarez, S., et al., 2014: Strong wintertime ozone events in the Upper Green River basin, Wyoming, *Atmos. Chem. Phys.*, 14, 4909–4934, doi:10.5194/acp-14-4909-2014.
- Schnell, R. C., Oltmans, S. J., Neely, R. R., Endres, M. S., Molenar, J. V., and White, A. B., 2009: Rapid photochemical production of ozone at high concentrations in a rural site during winter, *Nat. Geosci.*, 2, 120–122, doi:10.1038/ngeo415.
- Sillman, S. and He, D.: Some theoretical results concerning O<sub>3</sub>-NO<sub>x</sub>-VOC chemistry and NO<sub>x</sub>-VOC indicators, *J. Geophys. Res.*, 107, 4659, doi:10.1029/2001JD001123, 2002.